


STEAP3 Affects Ferroptosis and Progression of Renal Cell Carcinoma Through the p53/xCT Pathway

Technology in Cancer Research & Treatment
Volume 21: 1-9
© The Author(s) 2022
Article reuse guidelines:
sagepub.com/journals-permissions
DOI: 10.1177/15330338221078728
journals.sagepub.com/home/tct


Cheng Lin Ye, MS^{1,*} , Yang Du, MD^{1,*} , Xi Yu, MD¹,
Zhi Yuan Chen, MD¹, Lei Wang, MD¹, Yong Fa Zheng, MD¹,
and Xiu Heng Liu, MD¹

Abstract

Renal cell carcinoma is particularly sensitive to ferroptosis, an iron-dependent non-apoptotic form of cell death. This mechanism does not require activation of caspase or the participation of other apoptotic effector molecules (such as BAX or BAK), nor is it accompanied by the morphological characteristics or biochemical processes of apoptosis. The STEAP3 gene was found because it promotes tumor apoptosis in prostate cancer, but its role in renal cell carcinoma has not been studied in depth. Through real-time quantitative polymerase chain reaction, we found that the expression of the STEAP3 gene was upregulated in renal cell carcinoma tissue samples and cell lines, and it was found to be highly expressed in renal cell carcinoma tissue through immunohistochemistry. This upregulation is related to poor survival and prognosis of patients. We used erastin, a ferroptosis inducer, found that renal cell carcinoma became more susceptible to ferroptosis after knocking down STEAP3. The results indicate that renal cell carcinoma cell lines with knocked down STEAP3 expression are more sensitive to ferroptosis, and this effect occurs through the p53/xCT pathway. In summary, our research helps to identify new biomarkers and provides new targets for the treatment of renal cell carcinoma.

Keywords

ferroptosis, STEAP3, renal cell carcinoma, p53, xCT

Abbreviations

CAT, catalase; FBS, fetal bovine serum; OS, overall survival; PPI, protein–protein interaction; qRT-PCR, real-time quantitative polymerase chain reaction; RCC, renal cell carcinoma; ROS, reactive oxygen species; siRNA, small interfering RNA; SOD, superoxide dismutase; T-AOC, total antioxidant capacity.

Received: June 29, 2021; Revised: January 14, 2022; Accepted: January 19, 2022.

Introduction

Renal cell carcinoma (RCC) is a malignant tumor originating in the urinary tubule epithelial system of the renal parenchyma. It is the most common renal malignant tumor, accounting for approximately 80% to 90% of renal malignant tumors and approximately 2% to 3% of systemic malignant tumors. In 2019, there were approximately 73 820 new RCC cases in the United States and 14 770 deaths.¹ The incidence of RCC increases rapidly. The incidence of RCC is associated with obesity, and long-term intake of high-fat diets can induce RCC.² Although most of the lesions found are small tumors, a considerable number of patients are still diagnosed with locally advanced disease, and as many as 17% of patients have distant metastases at the time of diagnosis.³ Smoking is also

¹ Renmin Hospital of Wuhan University, Wuhan, Hubei Province, People's Republic of China

* Cheng Lin Ye and Yang Du are co-first authors and contributed equally in this paper.

Corresponding Authors:

Yong Fa Zheng, Renmin Hospital of Wuhan University, #99 Zhang Zhidong road, Wuhan 430060, Hubei Province, People's Republic of China.
Email: zyf0322@126.com

Xiu Heng Liu, Renmin Hospital of Wuhan University, #99 Zhang Zhidong road, Wuhan 430060, Hubei Province, People's Republic of China.
Email: drliuxh@hotmail.com



associated with the incidence of RCC, which includes a variety of carcinogens associated with the etiology of RCC.² The incidence of RCC has been increasing, patients often diagnosed with advanced RCC. In response, researchers are seeking new therapeutic targets and molecular markers.

Since ferroptosis was first proposed in 2012, research on tumors, ischemia–reperfusion, neurodegeneration, and other fields has continued to deepen.⁴ Ferroptosis is iron-dependent non-apoptotic cell death. This cell death mechanism does not require activation of caspase or the participation of other apoptotic effector molecules (such as BAX or BAK), nor is it accompanied by the morphological characteristics or biochemical processes of apoptosis. The morphology mainly includes a decrease in mitochondria, volume decrease, density increase, mitochondrial cristae decrease or disappearance, and mitochondrial outer membrane rupture.⁵ Yang *et al* found that RCC is particularly sensitive to ferroptosis regulated by GPX4.⁶ Lee *et al* found that overexpression of AMPK in the Caki-1 cells can protect cells from erastin-induced ferroptosis.⁷ Research on ferroptosis in RCC, especially renal clear cell carcinoma, continues to deepen. Ferroptosis is being studied as a treatment strategy that may help resolve the drug resistance of RCC.^{8,9}

STEAP3 is also known as pHyde or TSAP6. Previous studies by Steiner *et al* have shown that adenovirus-mediated STEAP3 expression can effectively inhibit the growth of prostate cancer *in vitro* and *in vivo* by inducing apoptosis and that STEAP3 mediates apoptosis with the participation of caspase-3; specifically, STEAP3 can increase the activity of caspase-3, and this increased caspase-3 activity can be blocked by its specific inhibitors DEVD and VAD.¹⁰ Passer observed that activation of endogenous P53 also increased the transcription of STEAP3 (STEAP3 transcripts were also increased by endogenous activation of p53).¹¹ Cells overexpressing STEAP3 were more sensitive to apoptosis, and NIX aggravated this effect. Studies by Shigehisa and Ning have shown that STEAP3 is highly expressed in RCC.^{12,13} This outcome was of particular interest to us. In this study, we aimed to determine why this apoptosis-promoting gene is highly expressed in RCC tissues and what effect it has on the development of RCC.

In the present study, we conducted a bioinformatics analysis based on renal clear cell carcinoma data in the TCGA database, followed by an examination of fresh renal clear cell carcinoma and paracancerous tissue samples. We found that STEAP3 is generally highly expressed in RCC. Combined with clinical data, we found that its high expression is an independent predictor of overall survival (OS). Further studies have shown that knockdown of RCC cell lines with high expression of STEAP3 increases sensitivity to ferroptosis and has an effect on biological behavior, and that this effect works through p53/xCT. Therefore, increasing the sensitivity of RCC cells to ferroptosis through STEAP3 targets has the potential to become a new method for the treatment of RCC.

Materials and Methods

Bioinformatics Analysis

The original data of RNA-seq were obtained from 610 renal clear cell carcinoma samples by TCGA, including 72 normal tissue

samples, 538 tumor tissue samples. Use DESeq2 for differential analysis, setting $P < .000001$, $\log_2\text{FoldChange} > 1$. Through the protein–protein interaction (PPI) analysis of 70 genes related to ferroptosis or iron metabolism through the string database and cytoHubba analysis, the top 10 Hub genes and their functional networks were obtained, and the differentially expressed mRNAs were selected for survival analysis. The ggsurv packets in R with $P < .05$ were used as the screening threshold in the survival analysis.

Patients and Tissue Samples

From January 2019 to November 2019, 34 fresh RCC and its adjacent tissues were obtained from the Department of Urology, Renmin Hospital of Wuhan University. All specimens were collected from patients who had received adjuvant radical resection and had informed consent. The specimen was diagnosed by 2 pathologists. This study was conducted under the permission of Institutional Ethics Committee of the Renmin Hospital of Wuhan University and in accordance with the “Ethical Management Guidelines.” The prior written consent is fully informed and signed by all participants.

Cell Lines and Cell Culture

Human RCC cell lines 786-O, A498, and normal renal tubular epithelial cell line HK-2 were obtained from American Type Culture Collection. OSRC-2 was obtained from Central Laboratory of Wuhan Renmin Hospital. The identification of these cell lines was conducted at the China Centre for Type Culture Collection. All cell lines were cultured in RPMI-1640 medium (HyClone) and supplemented with 10% fetal bovine serum (FBS) (Gibco) and 1% penicillin G sodium/streptomycin sulfate. All cells were grown in an incubator with 5% CO₂ at 37 °C. The small interfering RNA (siRNA) used for transfection was provided by Sangon Biotech. Transfections were performed according to the manufacturer’s instructions with RNAiMax transfection reagent (Thermo-Fisher Scientific).

Quantitative Real-Time PCR

RNA isolation was conducted using TRIzol reagent (Invitrogen). We used NovoStart® SYBR qPCR SuperMix Plus (Cat.E096-01A, Novoprotein, China) to perform real-time quantitative polymerase chain reaction (qRT-PCR). Fold increase was calculated with the $2^{-\Delta\Delta C_t}$ method. The sequences of the primers are as follows: STEAP3: 5'-TGCAAACCTCGCTCAACTGGAGG-3', 5'-AGGCAGGTAGAACTTGTAGCGG-3'; GAPDH: 5'-GTCTCC TCTGACTTCAACAGCG-3', 5'-ACCACCCTGTTGCTGTAGCC AA-3'. All samples were tested in triplicate and repeated 3 times.

Immunohistochemistry

Paraffin slices were sequentially dewaxed, hydrated, antigen retrieval, and antibody (anti-STEAP3, 1:50, 17186-1-AP, Proteintech) was used for 4 °C overnight. DAB was added to develop color, hematoxylin was used to redye, dehydrate, and

dry. Then film was sealed, photos were taken under microscope. The staining judgment method was based on the percentage of positive cells and the staining intensity. The STEAP3 expression score was defined as 0, 1, 2, and 3 according to the staining intensity, and the total staining score was low (0, 1) or high (2, 3). Two experienced pathologists, without knowing the clinical and pathological information of the samples, used the above scoring criteria to make the judgment and reached a consensus.

Protein Extraction and Western Blot Analysis

RIPA buffer solution was used to lyse RCC cells and extract total protein. The sample was placed on ice and subjected to ultrasonic cracking. The product was centrifuged for 15 min at 4 °C 12 000 rpm and supernatant was obtained. We used bicinchoninic acid (BCA) assay to measure protein concentration. The extracted protein was added to the loading buffer of 25% volume, heated for 10 min at 100 °C, and kept at -20 °C. Each sample was ran in 8% to 12% sodium dodecyl sulfate–polyacrylamide gel electrophoresis and then transferred to the polyvinylidene fluoride membrane (Millipore), then blocked with 5% nonfat milk for 1 h at room temperature, followed by incubation overnight at 4 °C with primary antibodies (anti-STEAP3, 1:2000, Proteintech, 17186-1-AP; anti-GPX4, 1:1000, Affinity, DF6701; anti-ACSL4, 1:1000, Affinity, DF12141; anti-XCT, 1:5000, Abcam, Ab175186; anti-p53, 1:5000, Proteintech, 60283-2-IG) and incubation at room temperature for 1 h with secondary antibody. Bands were detected by ChemiDoc Touch (Bio-Rad) and quantified with ImageJ software (W S Rasband, ImageJ, NIH).

Cell Biochemistry Assay and Reactive Oxygen Species Analysis

In this study, reduced glutathione assay kit was used to determine glutathione levels. The levels of catalase (CAT), total antioxidant capacity (T-AOC), superoxide dismutase (SOD) were measured using the CAT activity assay kit, T-AOC assay kit, and SOD assay kit. The level of lipid peroxidation was detected by MDA assay kit. The levels of reactive oxygen species (ROS) were detected using the MitoSOX Red Mitochondrial Superoxide Indicator. After the treatment, the cell homogenate (reagent provided with the kit) is centrifuged (1500 $g \times 10$ min, 25 °C) to remove the sediments. The supernatant was collected, added to the assay kit, and was tested at A412 (GSH), A520 (CAT), A593 (T-AOC), A450 (SOD), and A532 (MDA) by microplate reader.

Cell Counting Kit-8-Based Cell Viability Assay

RCC cells were inoculated into 96-well plates at the density of 2×10^3 cells/well, cultured for 24, 48, 72, and 96 h, each well was inoculated with 10 μ L cell counting kit-8 (CCK-8) reagent (CK04, Dojindo), then cultured for 1 h, the absorbance was determined at 450 nm. The cell growth curve was drawn according to the experimental results.

Tumor Cell Colony Formation Assay

Colony formation assay was used to detect clonogenicity of tumor cells. Cells were seeded into 6-well plates at about 200 cells per well and cultured for 10 days. Colonies were fixed in 3.7% paraformaldehyde for 15 min at 37 °C, stained with 0.1% crystal violet for 30 min at 37 °C, and counted manually.

Transwell Migration Assay

Twenty-four-well plate transwell chamber system (Corning) was used in transwell migration assay. In the upper chamber, 8×10^4 cells were suspended in 200 μ L serum-free medium, and in the lower chamber, 600 μ L 20% FBS medium was added to induce cell migration. After 72 h, the remaining cells in the upper lumen were removed with a cotton swab. When cells migrated to the other side of the membrane, it was fixed with 4% PFA for 30 min and stained with 0.1% crystal violet for 0.5 h.

Wound-Healing Assay

About 2 to 3×10^6 cells were inoculated into 6 well plates. When 90% to 95% cells fused, we scratched the cell layer with a sterile tip and washed 3 times with PBS. The cells were incubated for 0 h and 48 h, respectively. The test results were repeated in triplicate.

Statistical Analysis

All the experimental data were expressed by mean value \pm standard error of ≥ 3 independent experiments. We used Kaplan-Meier method to estimate the OS rate. The significance of the difference was compared with *t* test and χ^2 test. One-way analysis of variance was used to analyze the significant difference among groups. $P < .05$ was considered to be statistically significant.

Results

Key Differentially Expressed Genes Were Identified by Bioinformatics Analysis

Through differential expression analysis of 538 RCC samples from TCGA and 72 normal samples, 7 genes with low expression and 18 genes with high expression were obtained from 70 ferroptosis- and iron metabolism-related genes (Figure 1A). The highly expressed genes were SLC11A1, CP, TF, HMOX1, SLC39A14, HAMP, TFR2, SFXN3, HPX, HAVCR1, STEAP3, ABCB6, ABCG2, STEAP4, SLC25A37, ALAS2, CD163, and TMPRSS6, and the poorly expressed genes were FECH, ACO1, SFXN5, BMP6, SFXN2, SCARA5, and SLC48A1. We performed a PPI analysis of 70 genes associated with ferroptosis or iron metabolism in the STRING database using cytoHubba

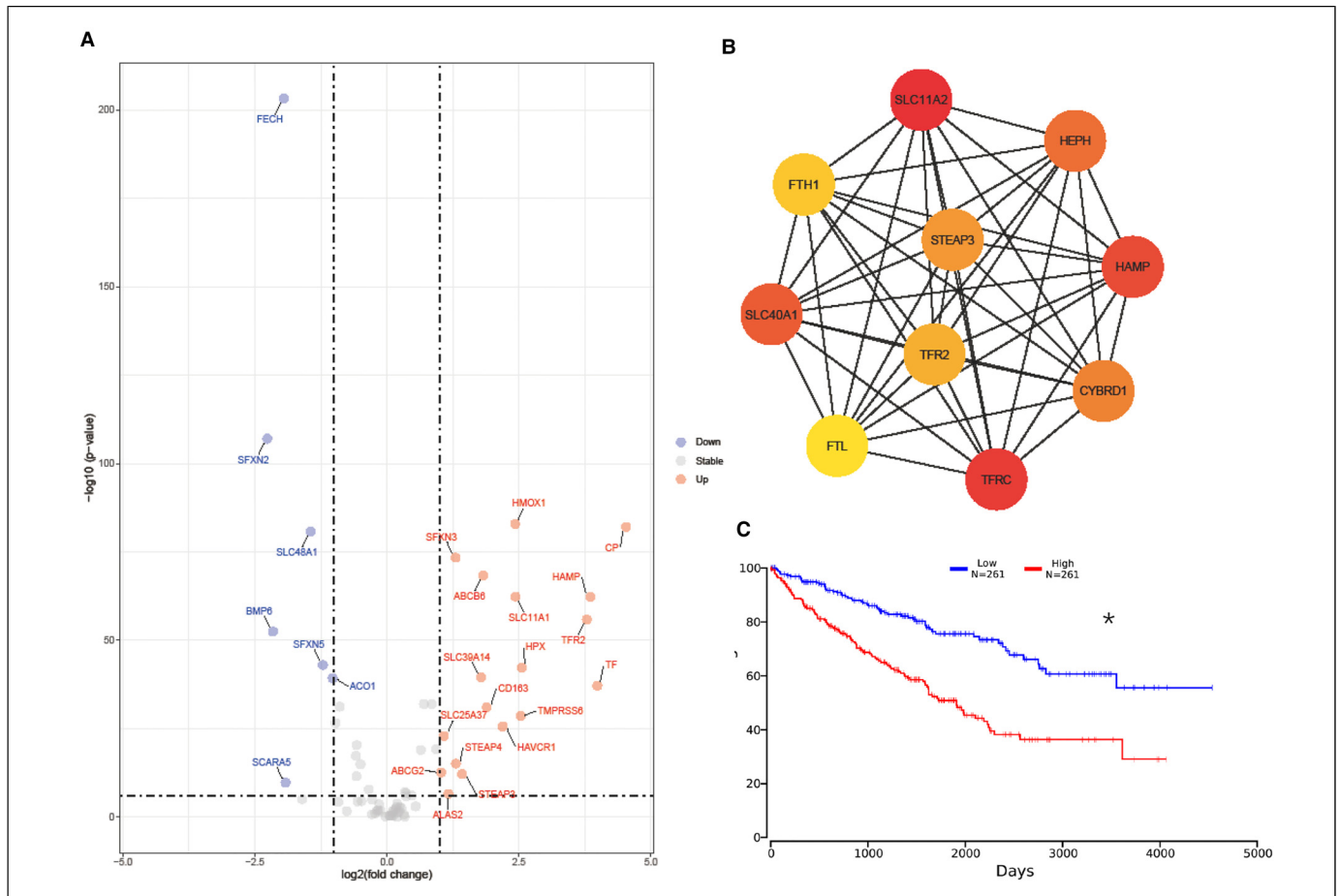


Figure 1. Differentially expressed genes in TCGA dataset, and survival analysis of STEAP3. (A) Volcano plot visualizing the all differentially expressed genes in TCGA dataset, (B) Through the protein–protein interaction (PPI) analysis of the String database and cytoHubba analysis, the top 10 Hub genes and their functional networks were obtained. (C) Through the analysis of clinical information of TCGA, patients with higher STEAP3 expression have poor prognosis.

to identify the top 10 hub genes and their interaction networks (Figure 1B). HAMP, STEAP3, and TFR2 were differentially expressed in 10 hub genes. We analyzed the clinical information on RCC samples in the TCGA database and found that patients with higher expression of STEAP3 had poorer prognoses (Figure 1C).

STEAP3 Is Highly Expressed in RCC Tissues and Cell Lines

We tested the mRNA expression of STEAP3 in RCC and adjacent tissues. qRT-PCR showed that mRNA expression in RCC samples was significantly higher than that in adjacent tissues (Figure 2A). The qRT-PCR results of RCC cell lines were consistent with tissues detection (Figure 2B). Results from Western blot verified the tendency of STEAP3 higher expression in tissue samples (Figure 2C) and cell lines (Figure 2D). Immunohistochemistry staining results (Figure 2E) showed increased levels of STEAP3 expression in RCC tissue samples.

Knockdown of STEAP3 Influences the Biological Behavior of RCC

We examined the inhibitory effect of siRNA. After transfection, the expression of STEAP3 protein and mRNA level was effectively inhibited (Figure 3A-C). The CCK-8 showed that after treatment with erastin, cell viability of the STEAP3 knockdown group was significantly lower than that of the control group (Figure 3D). Through cell colony formation assays (Figure 3E), wound-healing assays (Figure 3F), and Transwell invasion assays (Figure 3G), and after erastin, the STEAP3 knockdown group differed significantly from the control group. Our results suggest that knocking down STEAP3 can inhibit the development of tumors.

Knockdown of STEAP3 Increases the Sensitivity of RCC Cell Lines to Ferroptosis

The ferroptosis-related protein (p53 and ACSL4) expression in the STEAP3 knockdown group was higher than that in the non-knockdown group, while expression of other ferroptosis-related

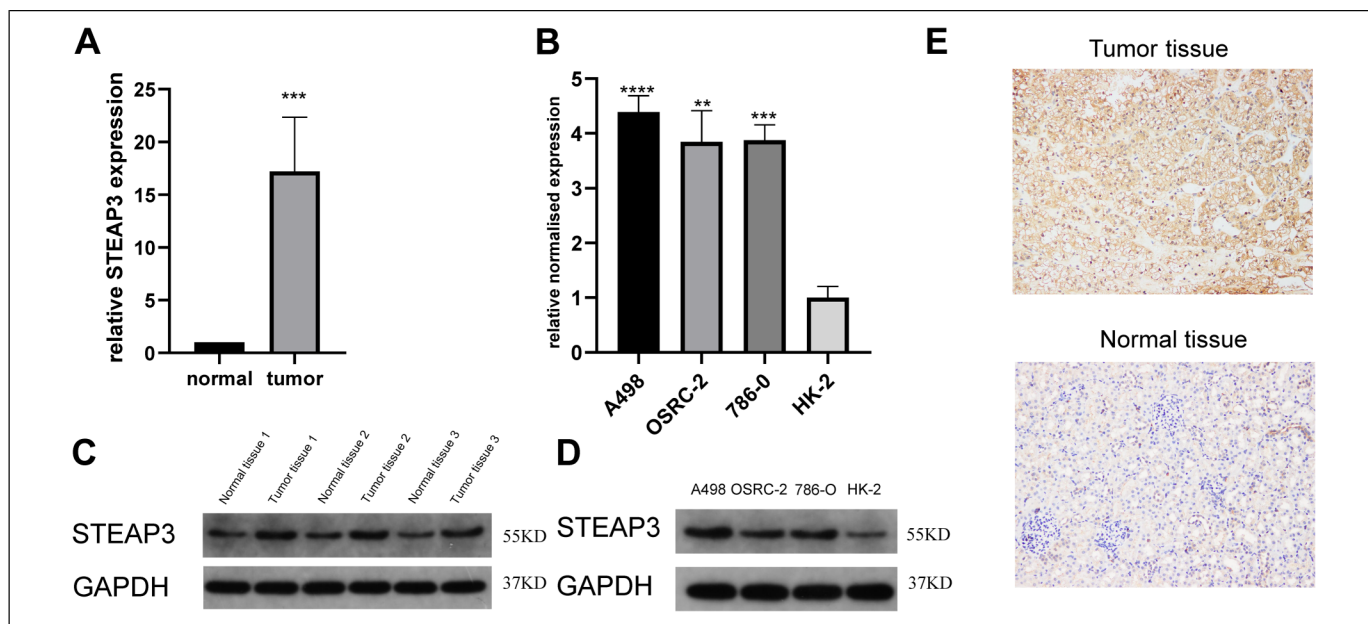


Figure 2. STEAP3 is highly expressed in kidney cancer tissues and cell lines. A, STEAP3 mRNA expression in renal cell carcinoma (RCC) was higher than that in adjacent tissues, which were normalized to control. (B) STEAP3 mRNA expression in kidney cancer cell lines (A498, OSRC-2786-O) was higher than normal renal cell line (HK-2) which was normalized to GAPDH. (C) STEAP3 protein had higher expression in tumor tissue in Western blot. (D) STEAP3 protein showed a higher expression in kidney cancer cell lines in Western blot. (E) Immunohistochemistry showed that STEAP3 protein had higher expression in tumor tissues. ** $P < .01$, *** $P < .001$, **** $P < .0001$.

protein (xCT and GPX4) decreased remarkably (Figure 4A and B). However, apoptosis-related protein, such as BCL-2, BAX had no changes (Figure S1). By measuring the intensity of the MitoSox probe signal in the cells, we measured the level of ROS in the cells. It was found that the STEAP3 knockdown group had a significant increase in ROS levels compared with the control group (Figure 4C). In the knockdown group, the expression of GSH, CAT, T-AOC, and SOD was decreased more than that in the control group, and the MDA concentration, which can reflect the degree of cell ferroptosis, increased more than that in the control group (Figure 4D and E). It has been proven that knocking down STEAP3 can increase the sensitivity of RCC cell lines to ferroptosis.

STEAP3 Affects Ferroptosis Sensitivity Through the p53/xCT Pathway

We observed the expression and activity of p53 and XCT in STEAP3-knockdown RCC cell lines and NC groups. We found that after knockdown of STEAP3 in RCC cell lines, the expression of p53 was upregulated and the expression of xCT was decreased compared to the control group (Figure 5A and B). Then, we used pifithrin (PFT)- α , a p53 inhibitor to determine whether the effect of STEAP3 knockdown could be rescued. As the result showed, PFT- α reversed the protein expression caused by STEAP3 knockdown (Figure 5A and B). To study the role of the p53/xCT pathway in STEAP3-mediated cell migration, proliferation, and invasion, we conducted rescue experiments. The CCK-8 showed that

after treatment with erastin, the cell viability of the STEAP3 knockdown group was significantly lower than that of the control group. In the presence of PFT- α , the changes in cell viability caused by the knockdown of STEAP3 can be rescued (Figure 5C). Transwell invasion showed that the invasion ability of cancer cells caused by the knockdown of STEAP3 can be rescued in the presence of PFT- α (Figure 5D). With the absence of erastin, GSH, CAT, T-AOC, SOD, and MDA which are affected by STEAP3 knockdown can be rescued by PFT- α (Figure S2).

Discussion

STEAP3 is a member of the 6-transmembrane epithelial antigen of prostate (STEAP) family, and they all have a common 6-transmembrane domain.¹⁴ STEAP3 was originally cloned from the mouse LTR6 cell line as a transcript induced by wild-type p53 activation.¹⁵ Steiner *et al* found that adenovirus-mediated STEAP3 gene expression can effectively inhibit the growth of prostate cancer *in vitro* and *in vivo* by inducing cell apoptosis.¹⁶ Studies by Ohgami and others have shown that STEAP3 can reduce Fe^{3+} in cells and can promote the absorption of ions by cells.^{14,17,18} Studies have shown that STEAP3 may be involved in cell apoptosis and cell cycle processes, especially the G2-M process.^{11,19,20} BCL2 interacting protein 3 like (BNIP3L also known as NIX) seems to enhance the apoptotic effect of STEAP3, and the interaction between STEAP3 and myelin transcription factor 1 (Myt1) implies the regulation of the phosphorylation state of Myt1.²¹ STEAP3 can be

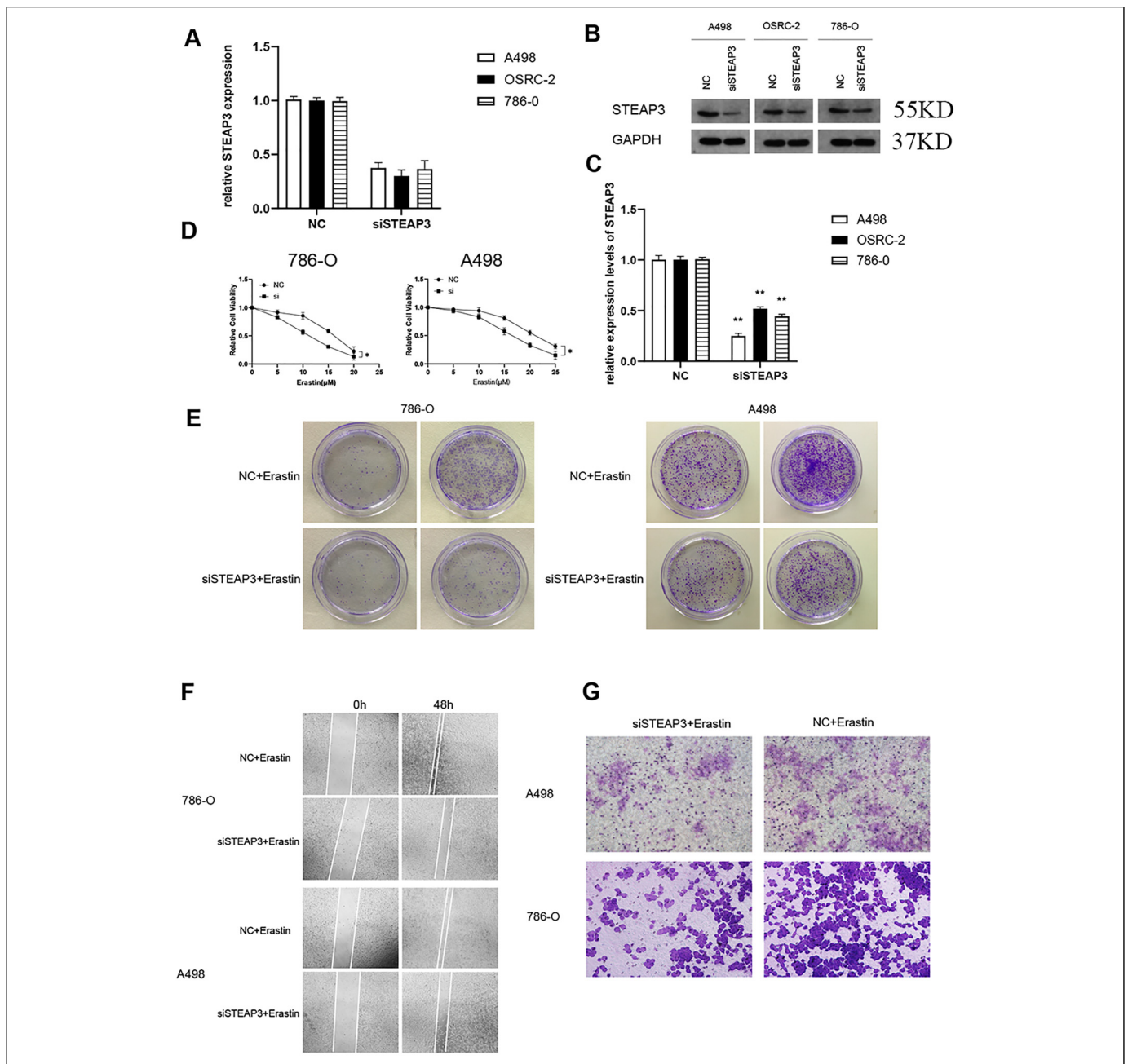


Figure 3. STEAP3 correlated with the sensitivity of kidney cancer cell lines to ferroptosis and can affect the biological behavior of the tumor. A, Confirmation of knockdown effect of STEAP3 in kidney cancer cell lines (A498, OSRC-2, 786-O) at mRNA level. STEAP3 mRNA was normalized to control. (B, C) Confirmation of knockdown effect of STEAP3 in kidney cancer cell lines (A498, OSRC-2, 786-O) at the protein level. STEAP3 protein level was normalized to control. (D) cell counting kit-8 (CCK-8) assays showed knockdown group had a higher susceptibility to ferroptosis than the NC group. (E) Colony formation assays showed that the knocking down of STEAP3 made kidney cell lines more sensitive to ferroptosis and decreased the proliferation capacity. Wound-healing assays (F) and transwell invasion (G) showed that STEAP3 affected the sensitivity of kidney cancer cell lines to ferroptosis and cell migration ability. The concentration of erastin is 10 μ M (786-O), 15 μ M (A498). All the above data are the mean \pm SD from an average of 3 experiments.

regarded as a positive regulator of Myt1, and STEAP3 and Myt1 together have a significant impact on the cell cycle and delay the G2-M process.¹¹ STEAP3 was first discovered in prostate cancer, and it can promote the apoptosis of prostate cancer. In colon cancer, lncRNA STEAP3-AS1 can modulate

cell cycle progression via affecting CDKN1C expression through STEAP3.²² In glioblastoma, STEAP3 predicts poor prognosis and promotes tumor growth and invasion.²³ STEAP3 is also associated with a transition from cirrhosis to hepatocellular carcinoma.²⁴ In this experiment, we verified

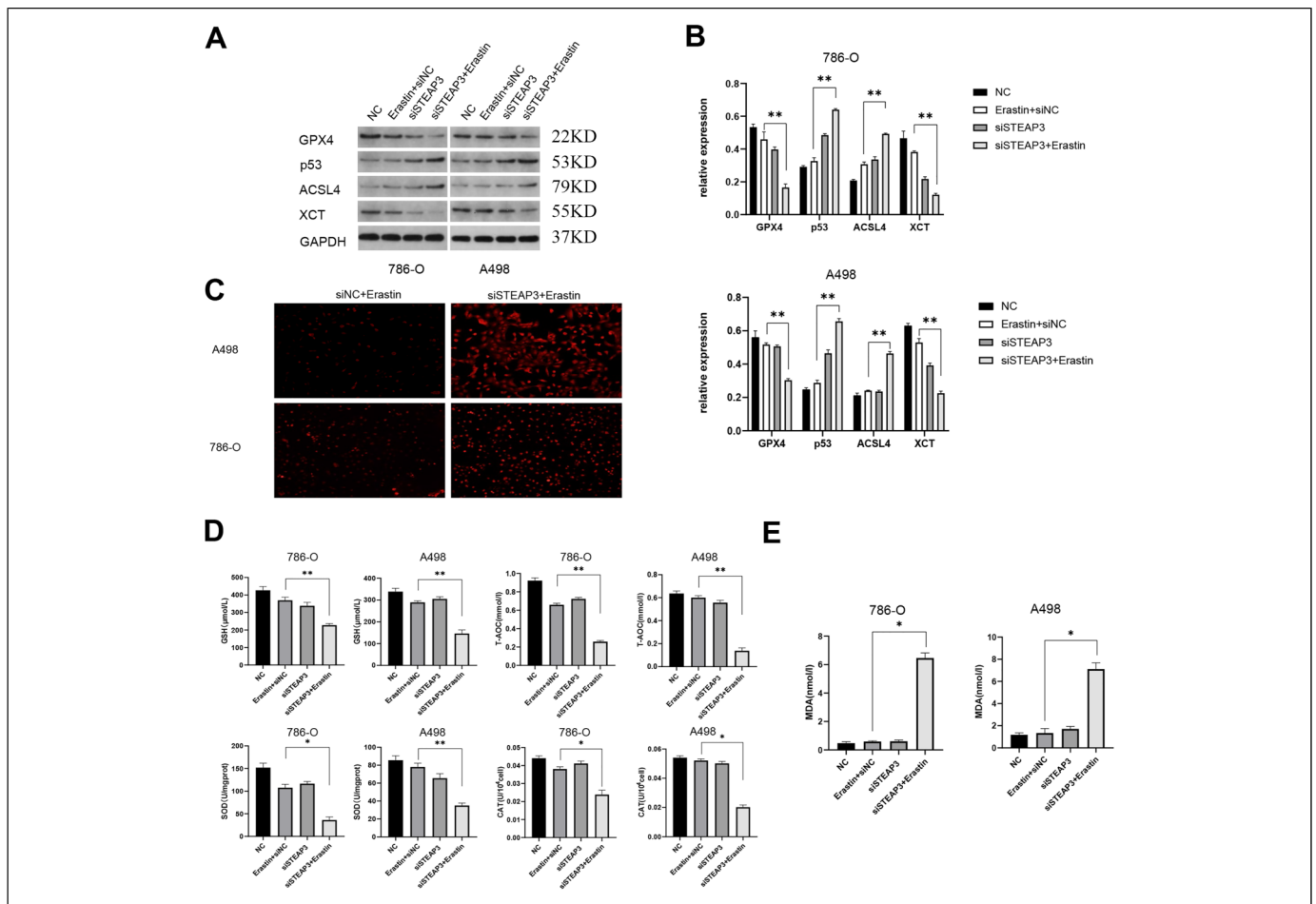


Figure 4. Changes in ferroptosis-related proteins, antioxidant capacity, and lipid peroxidation in 786-O and A498 cell lines. (A, B) Ferroptosis-related proteins were significantly different between siNC group and siSTEAP3 group when treated with erastin. The concentration of erastin is 10 μ M (786-O) and 15 μ M (A498). (C) MitoSox analysis of reactive oxygen species (ROS) levels in A498 and 786-O cells. (D) Quantification analysis of antioxidant markers in 786-O and A498 cells. (E) Quantification analysis of lipid peroxidation levels in HK-2 cells. All the above data are the mean \pm SD from an average of 3 experiments.

that STEAP3 is highly expressed in RCC tissues and cells, and through clinical information analysis, we found that its high expression is related to RCC. Our study provides genetic evidence that STEAP3 plays a key role in RCC. According to the analysis of clinical data, STEAP3 is an independent prognostic factor of RCC, and the expression of STEAP3 was negatively correlated with prognosis in RCC patients.

To further verify changes in the sensitivity of RCC cells to ferroptosis after knocking down STEAP3, we used erastin as an inducer and found that after knocking down STEAP3, erastin significantly reduced the antioxidant capacity of RCC cells, leading to increased lipid peroxidation and ROS levels. We can conclude that knocking down STEAP3 increases the sensitivity of RCC cells to ferroptosis. Then, we conducted a series of cell experiments and found that RCC cells after knocking down STEAP3 can significantly inhibit growth, migration, and invasion *in vitro* under the induction of erastin. We speculate that after knocking down STEAP3, the cystine/glutamate

transport system becomes more sensitive to the effects of erastin.

Inactivation of the P53 tumor suppressor pathway is a key event in the formation of most human cancers.^{25–28} Le *et al* inhibited SLC7A11 by transcription, a component of the cystine/glutamate antiporter, and p53 inhibited the uptake of cystine and made cells sensitive to ferroptosis, finding that p53-mediated transcriptional inhibition of SLC7A11 plays a key role in ROS-induced ferroptosis.²⁹ Brent *et al* found that STEAP3 transcripts are upregulated by p53 and that STEAP3 antisense impaired p53-mediated apoptosis, hinting at the possibility that STEAP3 may participate in cell death-related activities.¹¹ Our research found that STEAP3 and p53 expression was complementary, and the Western blot results showed that after knocking down STEAP3, the expression of p53 increased, and the expression of xCT downstream decreased. This is a good explanation for the increased sensitivity to ferroptosis of RCC cells caused by knockdown of STEAP3. The rescue experiment saved the effect of knocking down STEAP3. Our study

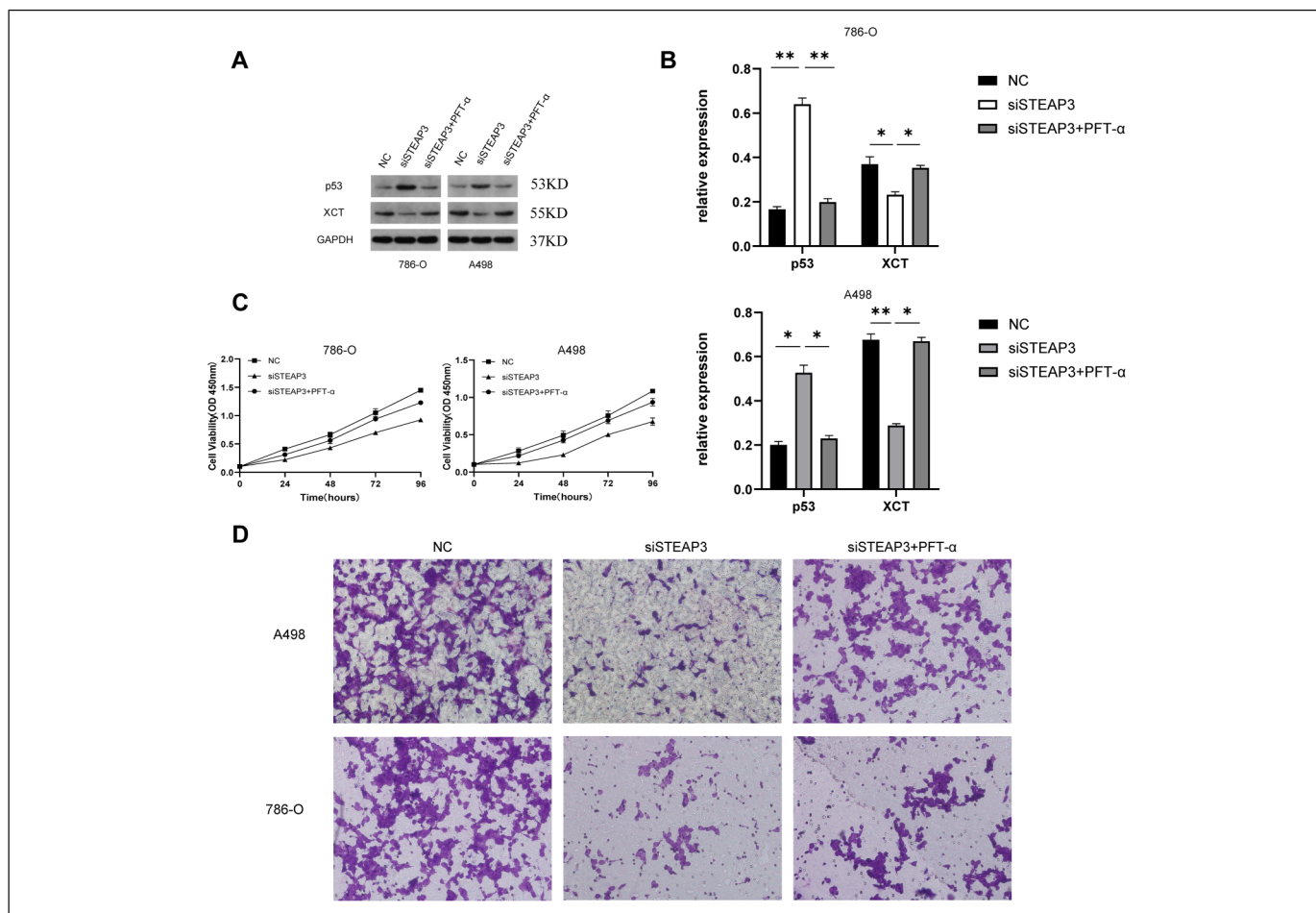


Figure 5. STEAP3 affects ferroptosis sensitivity through the p53/xCT pathway. (A, B) Knocking down of STEAP3 in 786-O and A498 cells, the expression of p53 was upregulated and the expression of xCT was decreased. PFT- α , an inhibitors of p53, could reverse it. (C, D) Cell counting kit-8 (CCK-8) assays and transwell invasion showed in the presence of PFT- α , the proliferation and invasion of siSTEAP3 kidney cancer cells(786-O, A498) were clearly elevated.786-O and A498 cells in CCK-8 assays and transwell were treated with erastin. The concentration of erastin is 10 μ M (786-O) and 15 μ M (A498).

demonstrated the important role of STEAP3 in RCC for the first time; STEAP 3 has the potential to be used as a biomarker to predict the survival of patients with RCC. STEAP3 may increase sensitivity to ferroptosis by regulating the p53/xCT pathway, thereby inhibiting tumor growth. Specifically, to determine whether knocking down the expression of STEAP3 can be used as a new strategy for the treatment of RCC, further study is warranted.

Authors' Note

Cheng Lin Ye and Yang Du contributed equally to this work. The present study was approved by The Ethics Committee of Renmin Hospital of Wuhan University. All patients provided written informed consent prior to enrollment in the study.

Declaration of Conflicting Interests

The author(s) declared no potential conflicts of interest with respect to the research, authorship, and/or publication of this article.



Funding

The author(s) disclosed receipt of the following financial support for the research, authorship, and/or publication of this article: This paper is funded by the National Natural Science Foundation of China (No. 81972408), the frontier project of Wuhan Applied Foundation (No. 2018060401011321).

Supplemental Material

Supplemental material for this article is available online.

ORCID iDs

Cheng Lin Ye  <https://orcid.org/0000-0002-2374-2790>
Yang Du  <https://orcid.org/0000-0002-3803-8245>

References

1. Siegel RL, Miller KD, Jemal A. Cancer statistics, 2019. *CA Cancer J Clin.* 2019;69(1):7-34.
2. Capitanio U, Bensalah K, Bex A, et al. Epidemiology of renal cell carcinoma. *Eur Urol.* 2019;75(1):74-84.

3. Capitanio U, Montorsi F. Renal cancer. *Lancet*. 2016;387-(10021):894-906.
4. Dixon SJ, Lemberg KM, Lamprecht MR, et al. Ferroptosis: an iron-dependent form of nonapoptotic cell death. *Cell*. 2012;149-(5):1060-1072.
5. Neiteimeier S, Jelinek A, Laino V, et al. BID links ferroptosis to mitochondrial cell death pathways. *Redox Biol*. 2017;12:558-570.
6. Yang WS, SriRamaratnam R, Welsch ME, et al. Regulation of ferroptotic cancer cell death by GPX4. *Cell*. 2014;156(1-2):317-331.
7. Lee H, Zandkarimi F, Zhang Y, et al. Energy-stress-mediated AMPK activation inhibits ferroptosis. *Nat Cell Biol*. 2020;22(2):225-234.
8. Yangyun W, Guowei S, Shufen S, Jie Y, Rui Y, Yu R. Everolimus accelerates erastin and RSL3-induced ferroptosis in renal cell carcinoma. *Gene*. 2021;809:145992.
9. Yang W-H, Ding C-KC, Sun T, et al. The hippo pathway effector TAZ regulates ferroptosis in renal cell carcinoma. *Cell Rep*. 2019;28(10):2501-2508.
10. Zhang X, Steiner MS, Rinaldy A, Lu Y. Apoptosis induction in prostate cancer cells by a novel gene product, pHyde, involves caspase-3. *Oncogene*. 2001;20(42):5982-5990.
11. Passer BJ, Nancy-Portebois V, Amzallag N, et al. The p53-inducible TSAP6 gene product regulates apoptosis and the cell cycle and interacts with Nix and the Myt1 kinase. *Proc Natl Acad Sci U S A*. 2003;100(5):2284-2289.
12. Kubota S, Yoshida T, Kageyama S, et al. A risk stratification model based on four novel biomarkers predicts prognosis for patients with renal cell carcinoma. *World J Surg Oncol*. 2020;18(1):270.
13. Zhao N, Huang Y, Wang Y-H, et al. Ferronostics: measuring tumoral ferrous iron with PET to predict sensitivity to iron-targeted cancer therapies. *J Nucl Med*. 2020;62(7):949-955.
14. Ohgami RS, Campagna DR, McDonald A, Fleming MD. The steap proteins are metalloreductases. *Blood*. 2006;108(4):1388-1394.
15. Amson RB, Nemani M, Roperch JP, et al. Isolation of 10 differentially expressed cDNAs in p53-induced apoptosis: activation of the vertebrate homologue of the drosophila seven in absentia gene. *Proc Natl Acad Sci U S A*. 1996;93(9):3953-3957.
16. Steiner MS, Zhang X, Wang Y, Lu Y. Growth inhibition of prostate cancer by an adenovirus expressing a novel tumor suppressor gene, pHyde. *Cancer Res*. 2000;60(16):4419-4425.
17. Ohgami RS, Campagna DR, Greer EL, et al. Identification of a ferrireductase required for efficient transferrin-dependent iron uptake in erythroid cells. *Nat Genet*. 2005;37(11):1264-1269.
18. Ohgami RS, Campagna DR, Antiochos B, et al. Nm1054: a spontaneous, recessive, hypochromic, microcytic anemia mutation in the mouse. *Blood*. 2005;106(10):3625-3631.
19. Aerbajinai W, Giattina M, Lee YT, Raffeld M, Miller JL. The proapoptotic factor Nix is coexpressed with Bcl-xL during terminal erythroid differentiation. *Blood*. 2003;102(2):712-717.
20. Liu F, Stanton JJ, Wu Z, Piwnicka-Worms H. The human Myt1 kinase preferentially phosphorylates Cdc2 on threonine 14 and localizes to the endoplasmic reticulum and Golgi complex. *Mol Cell Biol*. 1997;17(2):571-583.
21. Gomes IM, Maia CJ, Santos CR. STEAP Proteins: from structure to applications in cancer therapy. *Mol Cancer Res*. 2012;10-(5):573-587.
22. Na H, Li X, Zhang X, et al. lncRNA STEAP3-AS1 modulates cell cycle progression via affecting CDKN1C expression through STEAP3 in colon cancer. *Mol Ther Nucleic Acids*. 2020;21:480-491.
23. Han M, Xu R, Wang S, et al. Six-transmembrane epithelial antigen of prostate 3 predicts poor prognosis and promotes glioblastoma growth and invasion. *Neoplasia (New York, NY)*. 2018;20-(6):543-554.
24. Caillot F, Daveau R, Daveau M, et al. Down-regulated expression of the TSAP6 protein in liver is associated with a transition from cirrhosis to hepatocellular carcinoma. *Histopathology*. 2009;54-(3):319-327.
25. Berkers CR, Maddocks ODK, Cheung EC, Mor I, Vousden KH. Metabolic regulation by p53 family members. *Cell Metab*. 2013;18(5):617-633.
26. Jackson JG, Lozano G. The mutant p53 mouse as a pre-clinical model. *Oncogene*. 2013;32(37):4325-4330.
27. Aylon Y, Oren M. New plays in the p53 theater. *Curr Opin Genet Dev*. 2011;21(1):86-92.
28. Junttila MR, Evan GI. p53--a Jack of all trades but master of none. *Nat Rev Cancer*. 2009;9(11):821-829.
29. Jiang L, Kon N, Li T, et al. Ferroptosis as a p53-mediated activity during tumour suppression. *Nature*. 2015;520(7545):57-62.